Spatial Resolution and Minimum Detectability

36

CHAPTER PREVIEW

Often, when you do X-ray microanalysis of thin foils, you are seeking information that is close to the limits of spatial resolution. Before you carry out any such microanalysis you need to understand the various controlling factors, which we explain in this chapter. Minimizing your specimen thickness is perhaps the most critical aspect of obtaining the best spatial resolution, so we summarize the various ways you can measure your foil thickness at the analysis point.

A consequence of going to higher spatial resolution is that the X-ray signal comes from a much smaller volume of the specimen. A smaller signal means that we find it very difficult to detect the presence of trace constituents in thin foils. Consequently, the minimum mass fraction (MMF) in AEM is not very small compared with other analytical instruments which have poorer spatial resolution. This trade-off is true for any microanalysis technique, and so it is only sensible to discuss the ideas of spatial resolution in conjunction with analytical detectability limits. We'll make this connection in the latter part of the chapter. Despite the relatively poor MMF we can detect the presence of just a few atoms of one particular element if the analyzed volume is small enough, and so the AEM actually exhibits excellent minimum detectable mass (MDM) characteristics.

D. B. Williams et al., *Transmission Electron Microscopy*

Spatial Resolution and Minimum Detectability

36

36.1. WHY IS SPATIAL RESOLUTION IMPORTANT?

As we described in the introduction to Chapter 35, perhaps the major driving force for the development of X-ray microanalysis in the AEM was the improvement in spatial resolution compared with the EPMA. This improvement arises for two reasons:

- We use thin specimens, so less electron scatter occurs as the beam traverses the specimen.
- The higher electron energy (>100–400 keV in the AEM compared with 5–30 keV in the EPMA) further reduces scatter.

The latter effect occurs because the mean-free path for both elastic and inelastic collisions increases with the electron energy. The net result is that *increasing* the accelerating voltage when using thin specimens *decreases* the total beam–specimen interaction volume, thus giving a more localized X-ray signal source and a higher spatial resolution, as you can see in the Monte Carlo simulations in Figure 36.1A. Conversely, with bulk samples, *increasing* the voltage *increases* the interaction volume, and spatial resolution rarely improves below ~0.5 μm, as shown in Figure 36.1B. So no one is very interested in the theory of spatial resolution of microanalysis for bulk samples and little effort, beyond lowering the kV, is routinely made to optimize this parameter in practice. By contrast, much theoretical and experimental work has been carried out to both define and measure the spatial resolution of XEDS in the AEM, and we'll introduce some of the major ideas here.

36.2. DEFINITION OF SPATIAL RESOLUTION

We can define the spatial resolution of X-ray microanalysis as the smallest distance (R) between two volumes from which independent X-ray microanalyses can be obtained. The definition of R has evolved as AEMs have improved and smaller analysis volumes have become attainable. It has long been recognized that the analysis volume, and hence R, is governed by the beam–specimen interaction volume, since the XEDS can detect X-rays generated anywhere within that volume. The interaction volume is a function of the incident beam diameter (d) and the beam spreading (b) caused by elastic scatter of the beam within the specimen. Therefore, the measured spatial resolution is a function of your specimen, and this has made it difficult to define a generally accepted measure of R. Let's look first at d and b and how we define them.

We've already discussed how to define and measure d in TEMs and STEMs way back in Chapter 5, so you need only remind yourself that

> The beam diameter, d, is customarily defined as the FWTM of the Gaussian electron intensity. You can measure d directly from the TEM viewing screen, or indirectly by traversing the beam across a sharp edge and looking at the intensity change on the STEM screen.

This definition takes account of only 90% of the electrons entering the specimen, so it is an approximation. Remember that the intensity distribution in the incident beam is Gaussian only if you are careful in your choice and alignment of the C2 aperture. It is a little more diffi-

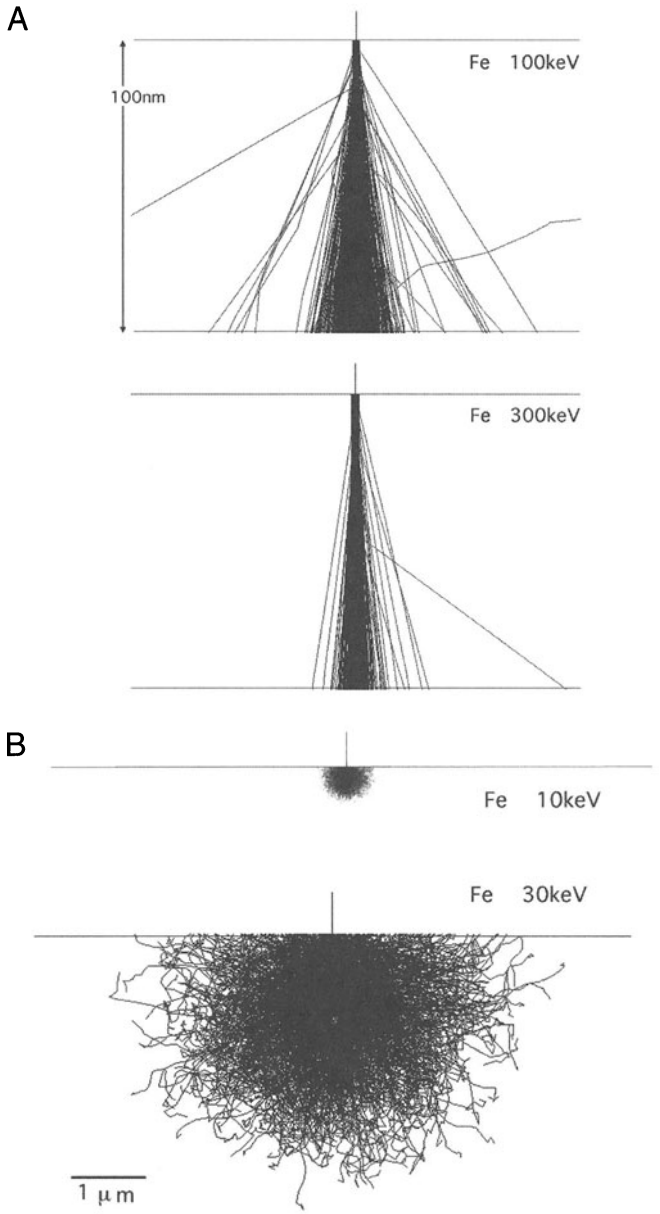

Figure 36.1. (A) Monte Carlo simulations of 10^3 electron trajectories through a 100-nm thin foil of Fe at 100 kV and 300 kV. Note the *improved* spatial resolution at higher kV. (B) Conversely, in a bulk sample the interaction volume at 30 kV is significantly more than at 10 kV, giving *poorer* X-ray spatial resolution at higher kV.

cult to define and measure b, so this needs more explanation.

36.3. BEAM SPREADING

The amount that the beam spreads on its way through the specimen (b) has been the subject of much theoretical and experimental work. While results and theories differ in minor aspects, there is a general consensus that b is governed by the beam energy (E_0), foil thickness (t), and density (ρ). It turns out that the most simple theory for b usually gives a good approximation under most microanalysis conditions. This theory, sometimes called the "single-scattering" model because it assumes that each electron only undergoes one elastic scattering event as it traverses the specimen, was first given in the seminal paper by Goldstein *et al.* (1977), and refined by Reed (1982). This single-scattering model states

$$b = 7.21 \times 10^5 \frac{Z}{E_0}\left(\frac{\rho}{A}\right)^{\frac{1}{2}} t^{\frac{3}{2}} \qquad [36.1]$$

This well-known expression is *not* in SI units because b and t are in given in cm, ρ is in g/cm^3, and E_0 is in eV.

This definition again comprises 90% of the electrons emerging from the specimen, so it is consistent with our definition of d.

There is some question as to whether this expression adequately describes the behavior of b for either very thin or very thick foils, but it has generally survived the test of time and its strength remains in its simplicity.

> We recommend that you keep this equation stored in your calculator or in the AEM computer system, so you can quickly estimate the expected beam spreading in your planned experiment.

You should, of course, estimate b *prior* to spending an inordinate amount of time trying to do an experiment which is impossible for lack of spatial resolution.

When we can't apply equation 36.1 (for example, if the specimen geometry or microstructure is complex) the best alternative is the Monte Carlo computer simulation (see Figure 36.1), which we introduced in Section 2.6 as a way of modeling electron scatter. Remember that the Monte Carlo technique uses a random number generator (hence the name) to simulate elastic and inelastic electron–specimen interactions and generate a feasible set of electron paths through a defined specimen. A relatively small number of paths (typically 10^3–10^6) can give a very good measure of the behavior of the very large number of electrons in a typical beam (remember, a 1-nA probe current implies ~10^{10} electrons/second entering the specimen). A full description is beyond the scope of this text and complete books exist on the topic (Heinrich *et al.* 1975, Joy 1995). After simulating several thousand paths, an approximate value of b can be obtained by asking the computer to calculate the diameter of a disk at the exit surface of the specimen that contains 90% of the emerging elec-

trons. This definition of b is consistent with that described at the start and is the dimension of b given by equation 36.1. In Joy's book, you'll find a code listing for a Monte Carlo simulation program which can be run on a PC. These simulations are now extremely rapid, and in a few minutes on a PC they can provide much of the information you need to estimate the beam spreading in heterogeneous microstructures that are not amenable to simple modeling with the single-scattering approach. Parallel supercomputers have even been used to simulate millions of trajectories in more complex specimens (Michael *et al.* 1993).

While beam spreading is the main aspect of spatial resolution theories, we mustn't forget that what we really want to know is the beam–specimen interaction volume, which corresponds to the X-ray source size. Of course this is closely related to the electron distribution, but we can only relate the two directly using Monte Carlo simulations. In these simulations you can easily get the computer to calculate the distribution of X-ray photons generated throughout the specimen, and factor it into any calculations of the composition of the analyzed volume. Monte Carlo simulations are useful for estimating the X-ray spatial resolution because they:

- Incorporate the effects of different kVs and beam diameters.
- Handle difficult specimen geometries and multiphase specimens.
- Automatically calculate the effect of the depth distribution of X-ray production $\varphi(\rho t)$ on the X-ray source size.
- Display the X-ray distribution generated anywhere in your specimen as a function of all its parameters, ρ, Z, A, and t. This tells you the relative contributions to your XEDS spectrum from different parts of the microstructure.

In addition to the theories of beam spreading that we've discussed, there are several more in the literature. A common feature of these theories is that they all predict a linear relationship between b and $t^{3/2}$ and an inverse relationship between b and E_0. If you're interested in the details of the various theories you'll find a discussion in Goldstein *et al.* (1986).

36.4. THE SPATIAL RESOLUTION EQUATION

Now that we've defined d and b, all we have to do is combine them to come up with a definition of R. Reed (1982) argued that if the incident beam was Gaussian, and if the beam emerging from the specimen retains a Gaussian intensity distribution, then b and d should be added in quadrature to give a value for R

$$R = \left(b^2 + d^2\right)^{\frac{1}{2}} \qquad [36.2]$$

This equation remained the standard definition of R for almost a decade, despite the fact that no set of experiments ever investigated the effects of all the variables affecting b in equation 36.1. About the same time as this definition of R was proposed, Gaussian beam-broadening models were introduced which were based on equation 36.1 but permitted convolution of the Gaussian descriptions of d and b to come up with a definition of R. Based on the Gaussian model and experimental measurements, Michael *et al.* (1990) proposed that the definition of R be modified so as not to present the worst case (given by the exit beam diameter) but to define R midway through the foil, as shown in Figure 36.2

$$R = \frac{d + R_{max}}{2} \qquad [36.3]$$

where R_{max} is given by equation 36.2.

This equation is the formal definition of the X-ray spatial resolution.

Like all definitions of spatial resolution, there is no fundamental justification for the choice of various factors

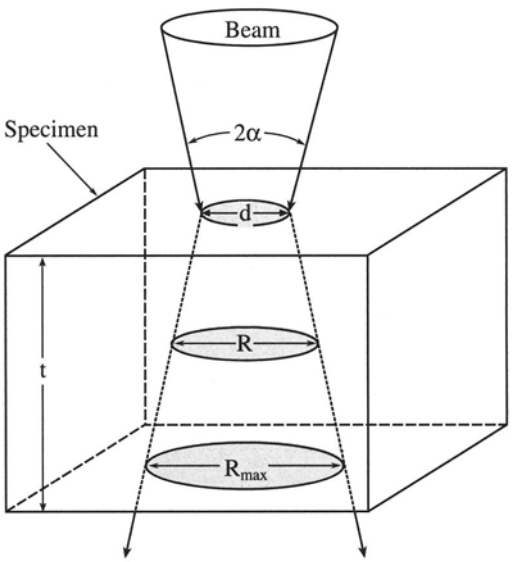

Figure 36.2. Definition of spatial resolution: schematic diagram of how the combination of incident beam size d and beam spreading through the foil combine to define the spatial resolution R of X-ray microanalysis in a thin foil.

such as the FWTM diameter, and the selection of the midplane of the foil at which to define R. Similarly, this approach ignores any contribution of electron diffraction in crystalline specimens, beam tailing beyond the 90% limit, and the effects of fast secondary electrons, which, in some circumstances, can be important. Nevertheless, the definition has been shown to be consistent with experimental results and sophisticated Monte Carlo simulations (Williams *et al.* 1992). Finally, this definition retains the advantage of the original single-scattering model, i.e., it has a simple form, easily amenable to calculation.

36.5. MEASUREMENT OF SPATIAL RESOLUTION

Any theory of spatial resolution must be tested against practical measurements in the TEM if it is to be relevant. Experimental measurements of the spatial resolution appeared slightly before the first theoretical treatments. Composition profiles measured across atomically sharp interphase interfaces were first presented by Lorimer *et al.* (1976). Since then, several other kinds of specimens have been proposed, such as spherical particles in a foil of known thickness, artificial specimens of Au lines deposited on a Si foil, grain boundary films, and quantum well structures, among others.

We believe the first method, using interphase interfaces, retains its validity since there are fewer unknowns than for the other specimens.

If thermodynamic equilibrium exists either side of the interphase interface, the solute content of each phase is well defined. Also, interphase interfaces are common to many engineering materials, as shown back in Figure 35.12.

In order to compare experimental and calculated measurements of R, you have to understand how we relate the measured composition profile across the interface to the actual discrete profile shape, shown schematically in Figure 36.3. We do this by deconvolution of the beam shape from the measured profile. The finite beam size, d, and the effect of b degrade the sharp profile to a width L, which is related to R by the following equation:

$$R = 1.414L \qquad [36.4]$$

Assuming this relationship holds, we just measure the distance L between the 2% and 98% points on the profile, as shown in Figure 36.3. This spread contains 90% of the beam electrons, consistent with our assumption of a 90%

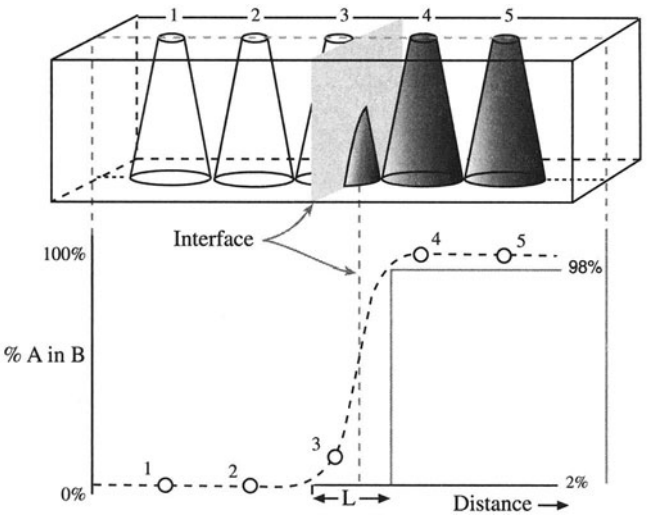

Figure 36.3. Schematic diagram showing the measured composition profile obtained across a planar interface at which an atomically discrete composition change occurs. The spatial resolution can be related to the extent (L) of the measured profile between the 2% and 98% points.

(FWTM) incident beam diameter. In practice, you will find it difficult to measure the 2% and 98% points because of the errors in the experimental data. So you should measure the distance from the 10% to the 90% points on your profile, corresponding to the beam spread containing 50% of the electrons (FWHM), then multiply this distance by 1.8 to give the FWTM.

Note that this definition of R, like the definitions of b and d that we have used, is arbitrary.

Nevertheless, it is easy to remember, relatively easy to measure, consistent with the definitions of b and d, and, most importantly, gives a number that is close to the experimentally measured degradation of the discrete composition change introduced by the beam and the specimen.

Typical measurements of the spatial resolution in two different AEMs are shown in Figures 36.4 and 36.5. Two composition profiles are shown. Each was taken from an Fe-Ni-Cr foil aged to give large Cr composition changes between Cr-rich α-Cr precipitates and the Cr-poor matrix. The specimen was aged sufficiently that the precipitate and matrix are in thermodynamic equilibrium, so that a discrete (atomic level) composition change occurs at the interface. The smooth profiles that appear in the figure are then due to the effects of b and d. In Figure 36.4, the data were obtained from an FEG AEM in which the accelerating voltage was kept constant at 100 kV and the specimen thickness

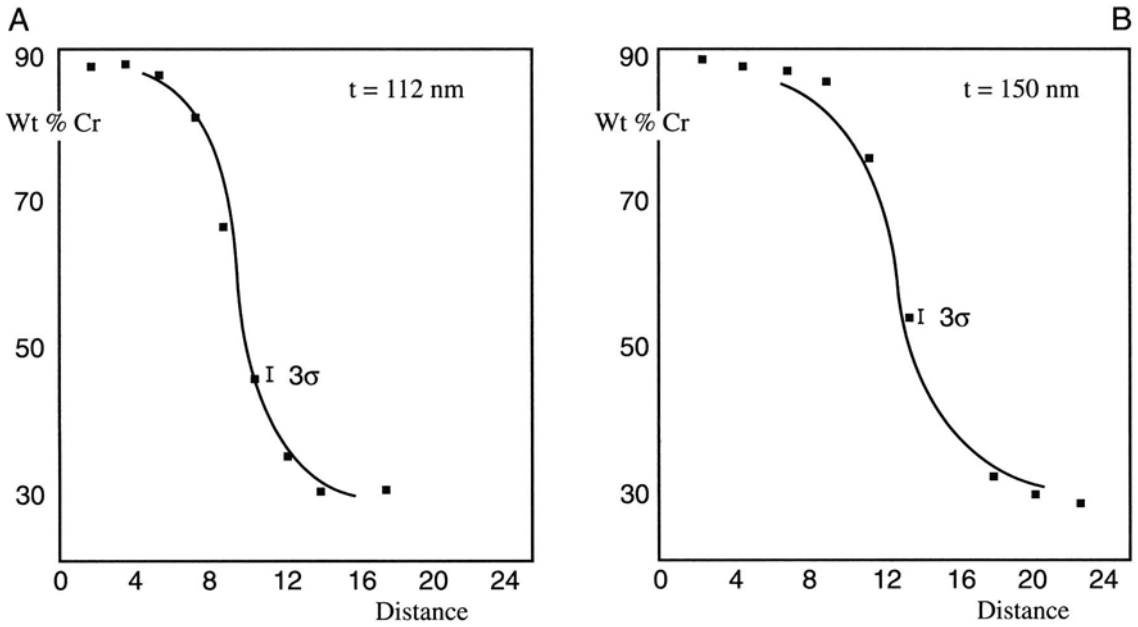

Figure 36.4. Measured Cr composition profiles across the same interface in an Fe-Ni-Cr alloy at two different thicknesses, (A) 112 nm and (B) 150 nm. The solid lines are the fits to the experimental data obtained using a Gaussian convolution model. The profiles were obtained in an FEG AEM at 100 kV and show that the $t^{3/2}$ relationship, assumed in the Gaussian model, applies over the range of thicknesses studied.

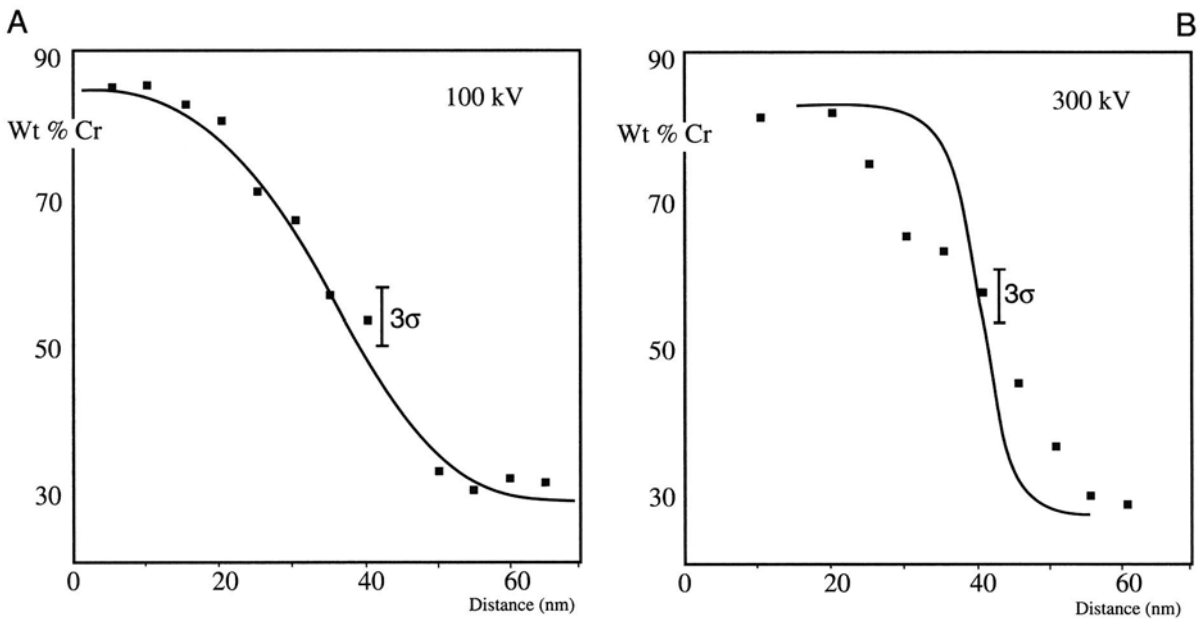

Figure 36.5. Composition profiles from an Fe-Ni-Cr foil, 112 nm thick, obtained with a thermionic source AEM at (A) 100 kV and (B) 300 kV. The solid lines are the fits obtained with a Gaussian convolution model and demonstrate poor spatial resolution, dominated by the large beam size. The bad fit at 300 kV indicates possible specimen drift.

was varied from 112 nm to 150 nm. In Figure 36.5, the data were obtained on an intermediate voltage AEM in which the foil thickness was a constant 120 nm but the voltage was varied between 100 kV and 300 kV. The line drawn through the experimental measurements in each case is derived from the Gaussian model.

It is obvious from equation 36.2 that if we want to improve spatial resolution, then both d and b must be minimized. But if we minimize d, we reduce the input beam current and, for thermionic sources, if d <10 nm, count rates are unacceptably low. However, with an FEG, sufficient current (~1 nA) can be generated in a 1-nm beam to permit quantitative analysis. Comparison of the 100-kV data from the thermionic source instrument (Figure 36.5A) and the FEG source (Figure 36.4A) shows the improvement gained by the use of very small beams in the FEG instrument.

So if you have a thermionic source AEM:

- Your specimen has to be thick enough that sufficient counts are generated for quantification and the net result may be that b is the main contributor to R.
- Alternatively, you may have to increase the beam size such that d dominates rather than b, as in Figure 36.5A (beam diameter 56 nm).

Such a large beam was needed in that example in order to generate sufficient beam current to get a reasonable X-ray count rate at 100 kV. This is one reason why there's been a lot of effort put into developing 300–400 kV AEMs and, more recently, 200–300 kV FEG AEMs.

There are some practical factors which can also limit your experimental spatial resolution:

- Specimen drift and carbon contamination are real problems with side-entry goniometer stages.
- Drift is often exacerbated by the liquid-N_2 cooling required to minimize carbon contamination.
- Changing the kV in intermediate voltage instruments subjects the objective lens cooling coil to large changes in thermal load, which causes drift.

Improvements in image analysis software mean that online drift correction is now available. If you're planning to carry out microanalysis at the highest spatial resolution where you're obliged to count for long times to accumulate adequate X-ray intensity, then such software is indispensable. Perhaps one unfortunate side effect of higher voltages is that analysis can be performed in thicker areas than at 100 kV and spatial resolution degrades.

In summary, the spatial resolution R is a function of both the beam size and the beam spreading. You can get a good estimate of R from equation 36.3. The theories all indicate a $t^{3/2}$ dependence of the beam spreading, so thin specimens are essential for the best resolution. FEG sources give sufficient beam current to generate reasonable counts even from very thin specimens and invariably give the best spatial resolution.

36.6. THICKNESS MEASUREMENT

Given the $t^{3/2}$ dependence of the beam spreading, you can see the importance of knowing t when estimating the spatial resolution. You already know that t is also an essential parameter in correcting for the absorption and fluorescence of characteristic X-rays, as we saw in the previous chapter. Furthermore, you should remember that knowledge of t is important in high-resolution phase-contrast imaging and CBED. You'll see in Chapter 39 that in EELS, minimizing t is again critical to obtaining the best results. In almost all TEM techniques your specimen has to be as thin as possible to get the best results; CBED studies are a notable exception to this generalization.

So let's take the opportunity here to summarize the methods available for measuring thickness. The methods are many and varied, and a full discussion of the most important techniques will be found in other parts of this book. The first point to remember is that the thickness we are interested in is t, the thickness through which the beam penetrates. This value depends both on the tilt of the specimen γ, and the true thickness at zero tilt, t_0. As shown in Figure 36.6, for a parallel-sided foil

$$t = \frac{t_0}{\cos \gamma} \qquad [36.5]$$

If your specimen is wedge-shaped, then t and t_0 will vary in an arbitrary fashion depending on the foil shape.

36.6.A. TEM Methods

In the TEM you can always make an estimate of your specimen thickness if it is wedge-shaped (and crystalline). By tilting to two-beam conditions for strong dynamical diffraction, the BF and DF images both show thickness fringes, as we saw in Chapter 23. These fringes occur at regions of constant thickness. The intensity in the BF image falls to zero at a thickness of $0.5\xi_g$ at $\mathbf{s} = 0$. Therefore, to determine t all you have to do is look at the BF image and count the number (n) of dark fringes from the edge of the specimen to the analysis region. At that point $t = (n - 0.5)\xi_g$, assuming that the thinnest part at the

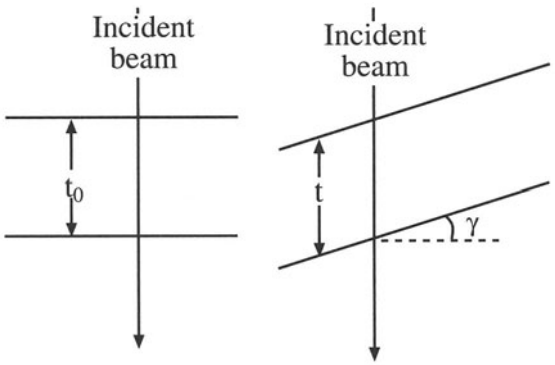

Figure 36.6. The difference between the specimen thickness, t_0, and the distance traveled by the beam, t, that determines beam spreading in a specimen tilted through an angle γ.

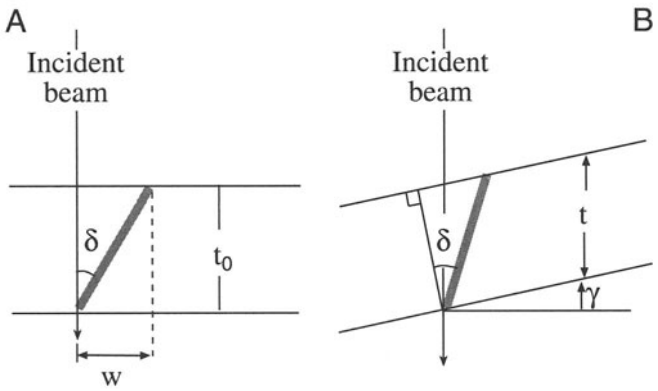

Figure 36.7. The parameters required to measure foil thickness t from a planar defect (projected width w), inclined to the incident beam by angle δ; comparison of (A) an untilted specimen normal to the beam and (B) a specimen tilted through an angle γ.

edge is $< 0.5\xi_g$ thick. (Be very careful with this assumption.) Remember that the value of ξ_g varies with diffracting conditions and so the **g**-vector has to be specified. You can calculate ξ_g from the expression

$$\xi_g = \frac{\pi \Omega \cos\theta}{\lambda f(\theta)} \qquad [36.6]$$

where Ω is the volume of the unit cell, λ is the electron wavelength, and $f(\theta)$ is the atomic scattering amplitude. Remember also that if you're not exactly at $\mathbf{s} = 0$, then the effective extinction distance ξ_{eff} must be used.

A related method relies on the presence of an inclined planar defect adjacent to the analysis region. The projected image of the defect, again under two-beam conditions, will exhibit fringes, which can be used to estimate the local thickness, or the projected width, w, of the defect image using the expression

$$t_0 = w \cot \delta \qquad [36.7]$$

as shown in Figure 36.7, in which δ is the angle between the beam and the plane of the defect. Again, you have to compensate geometrically to measure t rather than t_0 if the foil isn't normal to the beam, and then

$$t = w(\cot \delta - \tan \gamma) \qquad [36.8]$$

Of course both of these methods are inapplicable to noncrystalline materials, and it is not always possible to find a suitable inclined defect next to the analysis region. Furthermore, two-beam conditions are not recommended for microanalysis because of the dangers of anomalous X-ray emission (see Section 35.8). More insidious is the fact that oxidation, during or after specimen preparation, means that your crystalline specimen may be coated with an amorphous layer, which will not be measured by these diffraction-contrast techniques.

Another method related to the TEM image contrast involves measurement of the relative transmission of electrons. The intensity on the TEM screen decreases with increasing thickness, all other things being equal. Make all the intensity measurements on your specimen under the same diffraction conditions and incident beam current but with no objective aperture. By calibrating the intensity falling on the screen with a Faraday cup, you can get a crude measure of relative thickness, which can be converted into an absolute measure of t if some absolute method is used for calibration. The only advantage of this approach is that it is applicable to all materials, both amorphous and crystalline, but it is tedious and not very accurate.

Finally, an old method for thickness determination was to deposit small latex spheres on either side of your specimen and measure the thickness by noting parallax shifts between balls on the top and bottom sides as you tilt. This is not recommended, because the latex solution will contribute to specimen contamination and there are alternative and better methods. However, there are cases where you'll have particles or other markers already present on both surfaces, so you might use these for the parallax method.

36.6.B. Contamination-Spot Separation Method

This method, unique to a probe-forming (S)TEM, relies on the propensity of such instruments to generate carbon contamination on both the top and bottom surfaces of the specimen at the point of analysis. If you tilt your specimen by a

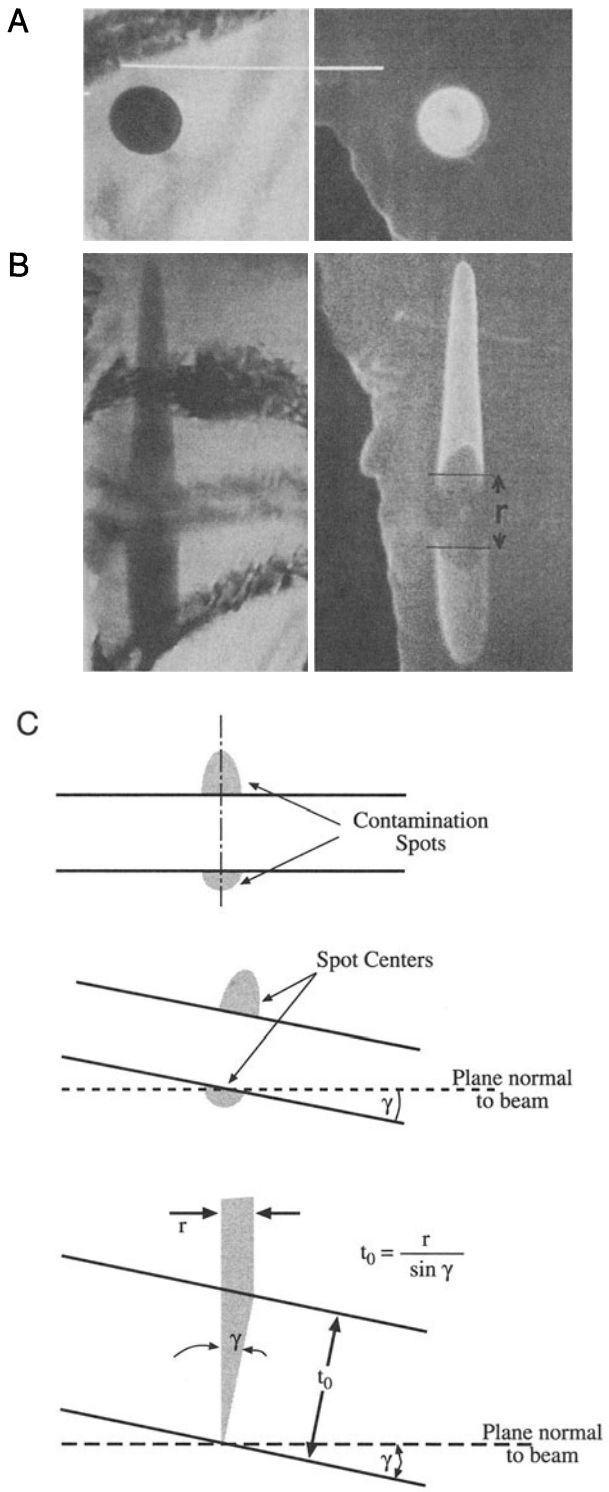

Figure 36.8. The contamination-spot separation method for thickness determination; (A) the contamination is deposited on both surfaces of the specimen and the separation (r) is only visible in (B) when the specimen is tilted sufficiently. The images show the contamination at zero tilt and high tilt angle γ. The two images on the left are obtained in STEM BF and on the right in SE mode. SE mode gives the best image contrast. (C) Geometry required to determine thickness t_0 from the projected spacing r of the contamination spots.

large enough angle γ, you can see discrete contamination spots (Figure 36.8). Their separation r, at a screen magnification M, is related to t_0 by the following expression

$$t_0 = \frac{r}{M \sin \gamma} \qquad [36.9]$$

If the specimen itself is tilted by an angle ε when the contamination is deposited, then

$$t_0 = \frac{r \cos \varepsilon}{M \sin \gamma} \qquad [36.10]$$

Although this method is straightforward, it relies on highly undesirable contamination, which obscures the very area you're looking at! Contamination degrades the spatial resolution and increases the X-ray absorption. In fact, we spend a lot of time and effort trying to minimize contamination, so it would be perverse to propose it as a useful way of determining t. Having said that, and despite ample evidence that the spot separation method overestimates the thickness by as much as 100%, it is often used because it is quick (and dirty!); it measures t exactly at the analysis point and the shape of the spots can indicate if the beam or the specimen has drifted during microanalysis. So if you can't avoid it, use it with caution.

36.6.C. X-ray Spectrometry Methods

Your X-ray spectrum intensity is a measure of the specimen thickness. Indeed, the standard method of quantification in biological materials uses the bremsstrahlung intensity as a measure of the mass thickness of the specimen, although this isn't used by materials scientists. If an element has two characteristic X-ray lines visible in the spectrum, e.g., the L and K lines, then the relative intensity of these lines will change as the specimen thickness increases because the lower-energy line will be more strongly absorbed. Knowing the necessary absorption parameters, such as μ/ρ, it is then possible to deduce ρt by an iterative process, which is essentially the same as the absorption correction discussed in Section 35.5. If ρ is known, then t can be determined. A similar method involves recording spectra containing an X-ray line that is strongly absorbed at two different tilts, or using two detectors with different take-off angles. In such cases, the two spectra will show different characteristic peak intensities because of the different absorption path lengths in each case. Again, an iterative process is required to extract t.

Porter and Westengen (1981) proposed such a method using standards, which still relies on an iterative procedure based on the absorption correction. In this method, the mass thickness is determined from the following equation

$$\rho t = \frac{\cos\gamma I_0(A)}{e_A m_A} \qquad [36.11]$$

where γ is the tilt angle, m_A is the mass fraction of element A in the specimen, e_A is the number of counts from element A detected per unit incident electron, per unit mass thickness of A in the absence of absorption, and $I_0(A)$ is the absorption-corrected intensity of A from the specimen. The calibration constant e_A is obtained from a standard of known mass thickness, such as a pure element foil. Since $I_0(A)$ is unknown, it is obtained from the absorption correction equation given by

$$I_0(A) = -\frac{\ln\left[1 - u_A I(A)\right]}{u_A} \qquad [36.12]$$

where $I(A)$ is the observed intensity of X-rays from element A and u_A is given by

$$u_A = \frac{\left(\frac{\mu}{\rho}\right)_{\text{Spec}}^{A} \operatorname{cosec}\alpha \cos\theta}{e_A m_A} \qquad [36.13]$$

You can write a similar equation for any element in your specimen. Thus, once your standard has been calibrated, the mass thickness can easily be calculated. However, as in all the absorption correction methods, an iterative process is required. If the foils are bent, or change thickness rapidly, then these methods all become very difficult to carry out and rather inaccurate. Furthermore, if e_A is to be a reliable calibration factor, the electron beam current must be stable and easily measurable; this isn't usually the case in the AEM.

Another closely-related method, described in Section 35.3 when we were discussing absorption, is the extrapolation technique in which the X-ray intensity is related directly to the mass thickness. So if you know the specimen composition you can obtain a value for t (Horita *et al.* 1989).

36.6.D. Electron Energy-Loss Spectrometry Methods

Thickness information is present in the electron energy-loss spectrum, since the intensity of inelastically scattered electrons increases with your specimen thickness. In essence, you have to measure the intensity under the zero-loss peak (I_0) and ratio this to the total intensity in the spectrum (I_T). The relative intensities are governed by the mean free path (λ) for energy loss. A parameterization formula for λ is discussed in detail in Section 39.5.

We can apply the EELS method to any specimen, amorphous or crystalline.

> EELS is applicable over a wide range of thicknesses, and with parallel-collection spectrometers it is so rapid that you can even produce thickness "maps" of thin foils. So this approach is highly recommended.

36.6.E. Convergent-Beam Diffraction Method

The CBED pattern, which is visible on the TEM screen when a convergent beam is focused on the specimen, can also be used to determine the thickness of crystalline specimens. In Section 21.1 we described the procedure to extract the thickness from the K-M fringe pattern obtained under two-beam conditions. The CBED pattern must come from a region thicker than $1\xi_g$ or else fringes will not be visible. Also, the region of the foil should be relatively flat and undistorted. We can envisage on-line thickness determination by digitizing the CBED pattern, scanning it across the STEM BF detector, and measuring the fringe spacing from the Y-modulation output on the STEM CRT. For clean crystalline specimens, this is *the* way to determine t.

In summary, there are many ways you can determine t, but no one method is convenient, accurate, and universally applicable. The various methods also measure different thicknesses, e.g., the crystalline thickness, neglecting surface films, or the thickness including surface films, or the mass thickness. The EELS, CBED, and X-ray absorption methods all have the possibility of widespread on-line use, and we recommend these methods, in order of preference. Detailed reviews of the methods of determining t have also been given by Berriman *et al.* (1984) and Scott and Love (1987).

36.7. MINIMUM DETECTABILITY

Minimum detectability is a measure of the smallest amount of a particular element that can be detected with a defined statistical certainty. Minimum detectability and spatial resolution are intimately related.

> It is a feature of any microanalysis technique that an improvement in spatial resolution is balanced by a worsening of the detectability limit (all other factors being equal).

At higher spatial resolution the analyzed volume is smaller, and therefore the signal intensity is reduced. This reduction

in signal intensity means that the acquired spectrum will be noisier and small peaks from trace elements will be less detectable. Accordingly, in the AEM, the price that you pay for improved spatial resolution is a relatively poor minimum detectability. By way of comparison, Figure 36.9 compares the size of the analyzed volume in an EPMA, a TEM/STEM with a thermionic source, and a dedicated STEM with an FEG. The enormous reduction in the beam–specimen interaction volume explains the small signal levels that we obtain in the AEM. It also explains why we have spent so much time emphasizing the need to optimize the beam current through use of higher brightness sources and modifying the specimen-detector configuration to maximize the collection angle, while minimizing the various sources of spurious radiation.

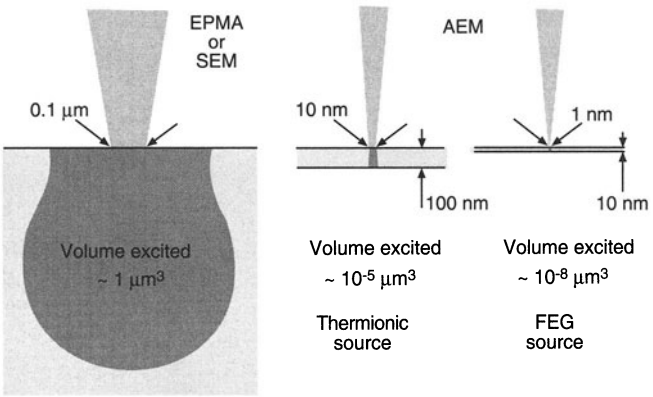

Figure 36.9. Comparison of the relative size of the beam–specimen interaction volumes in an EPMA, a thermionic source AEM, and an FEG-AEM with a bulk, thin, and ultrathin specimen, respectively.

We'll define the minimum detectability in terms of the minimum mass fraction (MMF), which represents the smallest concentration of an element (e.g., in wt.% or ppm) that can be measured in the analysis volume.

Alternatively, the minimum detectable mass (MDM) is sometimes used; the MDM describes the smallest amount of material (e.g., in mg) we can detect. We'll use the MMF, since materials scientists are more used to thinking of composition in terms of wt.% or at.%.

36.7.A. Experimental Factors Affecting the MMF

We can relate the MMF to the practical aspects of microanalysis through the expression of Ziebold (1967)

$$\text{MMF} \propto \frac{1}{\sqrt{P\frac{P}{B}n\tau}} \qquad [36.14]$$

Here, P is the X-ray count rate in the characteristic peak (above background) of the element of interest, P/B is the peak-to-background count-rate ratio for that peak (defined here in terms of the same width for both P and B), and τ is the analysis time for each of n analyses.

To increase P you can increase the current in the electron beam and/or increase the thickness (t) of the specimen. To increase P/B you can increase the operating voltage (E_0), which is easy, and decrease instrumental contributions to the background, which is not so easy (Zemyan and Williams 1994). Improvements in AEM instrument design, such as using a high-brightness and/or an intermediate voltage source, and a larger collection angle for the XEDS will also increase P. To increase P/B, you need a stable instrument with a clean vacuum environment to minimize or eliminate specimen deterioration and contamination. Improved AEM stage design, to minimize stray electrons and bremsstrahlung radiation, both of which contribute background to the detected spectrum, will also help to increase P/B, as we discussed back in Chapter 33.

Remember, however, that the Fiori definition of P/B is not the one used in Ziebold's equation (36.14) if you actually want to calculate the MMF.

The other variables in equation 36.14 are the time and number of analyses, which are entirely within your control as operator. Usually, both n and τ are a direct function of your patience and a 5–10 min coffee break is usually the maximum time for any one analysis. With computer control of the analysis procedure, however, there should be no limit to the time available for analysis. Particularly when detection of very small amounts of material is sought, τ should be increased to very long times. In the future, a period of several hours or overnight will not be considered unreasonable. Of course, the investment of so much time in a single analysis is dangerous unless you have judiciously selected the analysis region, and you are confident that the time invested will be rewarded with a significant result. Obviously you should minimize factors that degrade the quality of your analysis with time, such as contamination, beam damage, and specimen drift. Therefore, you should only carry out long analyses if your TEM is clean (preferably UHV) and your specimen is also clean and stable under the beam. Any specimen drift must be corrected by computer control during the analysis.

36.7.B. Statistical Criterion for the MMF

We can also define the MMF by a purely statistical criterion. We discussed back in Chapter 34 that we can be sure a peak is present if the peak intensity is greater than three

times the standard deviation of the counts in the background under the peak. From this we can come up with a definition of the detectability limit which, when combined with the Cliff–Lorimer equation (assuming Gaussian statistics), gives the MMF (in wt.%) of element B in element A as

$$C_B(\text{MMF}) = \frac{3\left(2\,I_B^b\right)^{\frac{1}{2}} C_A}{k_{AB}\left(I_A - I_A^b\right)} \qquad [36.15]$$

where I_A^b and I_B^b are background intensities for elements A and B, I_A is the raw integrated intensity of peak A (including background), C_A is the concentration of A (in wt.%), and k_{AB} is the Cliff–Lorimer factor. However, if we express the Cliff–Lorimer equation as

$$\frac{C_A}{k_{AB}\left(I_A - I_A^b\right)} = \frac{C_B}{\left(I_B - I_B^b\right)} \qquad [36.16]$$

and substitute it into equation 36.15, the MMF is

$$C_B(\text{MMF}) = \frac{3\left(2\,I_B^b\right)^{\frac{1}{2}} C_B}{I_B - I_B^b} \qquad [36.17]$$

Experimentally, low count-rates from thin specimens mean that typical values of MMF are in the range 0.1% to 1%, which is rather large compared with some other analytical techniques. The best compromise in terms of improving MMF while maintaining X-ray spatial resolution is to use high operating voltages (300 to 400 kV) and thin specimens to minimize beam broadening. The loss of X-ray intensity, a consequence of using thin specimens, can be compensated in part by the higher voltages and/or by using an FEG where a small spot size of 1 to 2 nm can still be maintained. In summary, optimum MMF and spatial resolution can be obtained by using a high-brightness, intermediate voltage source with thin foils, perhaps of the order of $t \sim 10$ nm. Under these circumstances, MMF values <0.1 wt.% will become routine. Figures 36.9 and 36.10 summarize the classic compromise between resolution and detectability (Lyman 1987).

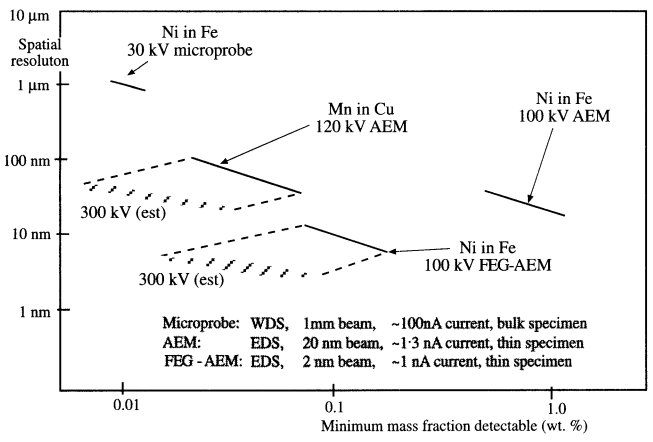

Figure 36.10. Calculation of the relationship between MMF and spatial resolution for the EPMA and a range of AEMs. The inverse relationship between the MMF and resolution is clear, although it is also apparent that the high-brightness sources and high-kV electron beams in the AEM can compensate for the decreased interaction volume in a thin foil.

36.7.C. Comparison with Other Definitions

The MMF definition is not the only way we can measure detectability limits. Currie (1968) has noted at least eight definitions in the analytical chemistry literature. Currie defined three specific limits:

- The decision limit (L_c): Do the results of your analysis indicate detection or not?
- The detection limit (L_d): Can you rely on a specific analysis procedure to lead to detection?
- The determination limit (L_q): Is a specific analysis procedure precise enough to yield a satisfactory quantification?

For I_B counts from element B in a specific peak window and I_B^b in the background, it can be shown that

$$L_C = 2.33\sqrt{I_B^b} \qquad [36.18]$$

$$L_d = 2.71 + 4.65\sqrt{I_B^b} \qquad [36.19]$$

$$L_q = 50\left\{1 + \left(1 + \frac{I_B^b}{12.5}\right)^{\frac{1}{2}}\right\} \qquad [36.20]$$

If there are sufficient counts in the background

$$L_d = 4.65\sqrt{I_B^b} \qquad \text{when } I_B^b > 69 \qquad [36.21]$$

$$L_q = 14.1\sqrt{I_B^b} \qquad \text{when } I_B^b > 2500 \qquad [36.22]$$

Comparison of these definitions with the statistical criterion in the previous section shows that $C_{MMF} \approx L_d$. So if you want to quantify an element, not just determine that it is present (L_d), then you need substantially more (~3×) of the element in your specimen (Zemyan 1995). Rather than do the experiment yourself, it is possible to simulate spectra from small amounts of element B in A (or vice versa), using DTSA. We recommend that you simulate your analysis before embarking on a time-consuming experiment which may be futile, because the amount of the element you are seeking is below the MMF.

36.7.D. Minimum Detectable Mass

The MMF values may seem poor compared with other analytical techniques which report ppm or ppb detectability limits. However, it's a different matter if you calculate what the MMF translates to in terms of the minimum detectable mass (MDM).

> The MDM is the minimum number of atoms detectable in the analyzed volume.

Using data for the MMF of Cr in a 304L stainless steel measured in a VG HB-501 AEM with an FEG, Lyman and Michael (1987) obtained an MMF of 0.069 wt.% Cr in a 164-nm foil with a spatial resolution of 44 nm and a 200-s counting time. The electron beam size was 2 nm (FWTM) with a beam current of 1.7 nA. In this analysis, an estimated 2×10^4 atoms were detected and the MDM was less than 10^{-19} g. If the counting time is increased by a factor of 10 and the operating voltage is increased to 300 kV, the spatial resolution would improve to ~15 nm and the MMF would improve to ~0.01 wt.%. Thus about 300 atoms could be detected. For a foil thickness of 16 nm (1/10th the above measured thickness), the MMF would degrade to ~0.03 wt.%. However, the spatial resolution would improve to about 2 nm. For this case, about 20 atoms would be detected corresponding to less than 10^{-22} g, which is an amazing figure by any standards. Therefore in ~10-nm-thick specimens, with a spatial resolution approaching the beam diameter d, of 1 to 2 nm, we will be able to detect the presence of 10 to 100 atoms in the analysis volume (10^{-8} μm^3); preliminary data reporting <10 atoms have been published (Lyman *et al.* 1994). For comparison, in the EPMA with 1 μm^3 excitation volume and a 0.01 wt.% MMF, ~10^7 atoms are detected in the analysis volume.

CHAPTER SUMMARY

You cannot optimize spatial resolution and minimum detectability in the same experiment. You must decide which of the two criteria is more important for the result you're seeking:

- To get the best spatial resolution, operate with the thinnest foils and the highest-energy electron beam. Use an FEG if possible.
- To measure the specimen thickness, use the parameterized EELS approach, otherwise choose between any of the several X-ray intensity methods, or CBED for a crystalline foil.
- To get the best MMF, use the brightest electron source, or the largest beam and thickest specimen, and count for as long as possible.
- If you want the best resolution *and* MMF, an FEG is essential, along with a clean specimen and computer-controlled drift correction; patience is also desirable.

REFERENCES

General References

Berriman, J., Bryan, R.K., Freeman, R., and Leonard, K.R. (1984) *Ultramicroscopy* **13**, 351.

Goldstein, J. I., Williams, D.B., and Cliff, G. (1986) in *Principles of Analytical Electron Microscopy* (Eds. D.C. Joy, A.D. Romig Jr., and J.I. Goldstein), p. 155, Plenum Press, New York.

Scott, V.D. and Love, G. (1987) *Mat. Sci. Tech.* **3**, 600.

Specific References

Currie, L.A. (1968) *Anal. Chem.* **40**, 586.

Goldstein J.I., Costley, J.L., Lorimer, G.W., and Reed, S.J.B. (1977) *Scanning Electron Microscopy*, **1** (Ed. O. Johari), p. 315, IITRI, Chicago, Illinois.

Heinrich, K.F.J., Newbury, D.E., and Yakowitz, H., Eds. (1975) NBS Special Publication 460, U.S. Dept. of Commerce, Washington, D.C.

Horita, Z., Ichitani, K., Sano, T., and Nemoto, M. (1989) *Phil. Mag.* **A59**, 939.

Joy, D.C. (1995) *Monte Carlo Modeling for Electron Microscopy and Microanalysis,* Oxford University Press, New York.

Lorimer, G.W., Cliff, G., and Clark, J.N. (1976) in *Developments in Electron Microscopy and Analysis* (Ed. J.A. Venables), p. 153, Academic Press, London.

Lyman, C.E. (1987) in *Physical Aspects of Microscopic Characterization of Materials* (Eds. J. Kirschner, K. Murata, and J.A. Venables), p. 123, *Scanning Microscopy International,* AMF O'Hare, Illinois.

Lyman, C.E. and Michael, J.R. (1987) in *Analytical Electron Microscopy-1987* (Ed. D.C. Joy), p. 231, San Francisco Press, San Francisco, California.

Lyman, C.E., Goldstein, J.I., Williams, D.B., Ackland, D.W., Von Harrach, S., Nicholls, A.W., and Statham, P.J. (1994) J. *Microsc.* **176**, 85.
Michael, J.R., Williams, D.B., Klein, C.F., and Ayer, R. (1990) *J. Microsc.* **160**, 41.
Porter, D.A. and Westengen, H. (1981) in *Quantitative Microanalysis with High Spatial Resolution* (Eds. M.H. Jacobs, G.W. Lorimer, and P. Doig), p. 94, The Metals Society, London.
Reed, S.J.B. (1982) *Ultramicroscopy* 7, 405.
Williams, D.B., Michael, J.R., Goldstein, J.I., and Romig, A.D. Jr. (1992) *Ultramicroscopy* **47**, 121.
Zemyan, S.M. (1995) Ph.D. dissertation, Lehigh University.
Zemyan, S.M. and Williams, D.B. (1994) *J. Microsc.* **174**, 1.
Ziebold, T.O. (1967) *Anal. Chem.* **39**, 858.